

Supporting Information for

A Bi(III)-based halide with near-unity photoluminescence quantum

yield as blue-light-excited red phosphor for WLED

Dan-Dan Huang,^{a,b,d} Abdusalam Ablez,^{a,b,d} Ting-Hui Zhuang,^b Hao-Wei Lin,^{a,d} Zhong-Hua Deng,^a Ke-Zhao Du,^{c*} Ze-Ping Wang,^{a*} and Xiao-Ying Huang^{a,d*}

^a State Key Laboratory of Structural Chemistry, Fujian Institute of Research on the Structure of Matter, Chinese Academy of Sciences, Fuzhou, Fujian 350002, P. R. China.

^b College of Chemistry, Fuzhou University, Fuzhou 350108, P. R. China.

^c Fujian Provincial Key Laboratory of Advanced Materials Oriented Chemical Engineering, Fujian Normal University, 32 Shangsang Road, Fuzhou 350007, P. R. China.

^d Fujian College, University of Chinese Academy of Sciences, Fuzhou 350002, P.R. China.

E-mail: xyhuang@fjirsm.ac.cn

E-mail: duke@fjnu.edu.cn

E-mail: wzping520@msn.cn

Experimental

Materials and methods. The detailed information for the reagents is listed as follows: Benzyltriphenylphosphonium bromide ([BzPPh₃]Br, 98%, Adamas Reagent Co., Ltd., Shanghai, China); bismuth(III) bromide (BiBr₃, 98%, Adamas Reagent Co., Ltd., Shanghai, China); 4,4'-bipyridine 1,1'-dioxide hydrate (bp4do·H₂O, 97%, Jinan Henghua Sci. & Tec. Co., Ltd., Shandong, China); dimethyl sulphoxide (DMSO, AR, Sinopharm Chemical Reagent Co., Ltd., Shanghai, China); ethanol (EtOH, AR, Sinopharm Chemical Reagent Co., Ltd., Shanghai, China). All purchased reagents were utilized directly without further purification.

Characterizations. Powder X-ray diffraction (PXRD) patterns were measured on a Rigaku Miniflex-II diffractometer by utilizing MoK_α radiation ($\lambda = 0.71073 \text{ \AA}$) in the angular range of $2\theta = 5\text{--}65^\circ$.¹ Thermogravimetric (TG) analyses were performed on a NETZSCH STA 449F3 unit at a heating rate of 10 K·min⁻¹ under N₂ atmosphere. Photoluminescence excitation (PLE) and photoluminescence (PL) spectra and time-resolved PL spectra and quantum yields of compound **Bz-BiBrON** were recorded on Edinburgh FLS1000 UV/V/NIR fluorescence spectrometer. EA was performed on a German Elementary Vario MICRO instrument.

Syntheses. **Bz-BiBrON** samples were prepared by hand milling method. A mixture of BiBr₃ (2 mmol, 0.8961 g), bp4do·H₂O (1 mmol, 0.1882 g), [BzPPh₃]Br (2 mmol, 0.8662 g), and DMSO (1 mL) was added to a mortar and ground for one minute. The sample was then washed several times with EtOH and dried to obtain an orange-yellow powder sample. The calculated yield based on bp4do was close to 96%. EA: Calcd (%): C, 35.98; H, 3.10; N, 1.11. Found (%): C, 36.06; H, 3.13; N, 0.99.

[BzPPh₃]₂[Bi₂Br₈(bp4do)_{0.833}(DMSO)_{2.33}]. Single crystals of **Bz-BiBrON** were prepared by slow evaporation method. Weighing 0.1 g of the powder dissolved in 2 mL DMSO and slow evaporation of DMSO for several weeks gave orange bulk crystals.

Single Crystal X-ray Diffraction (SCXRD). A suitable single crystal was selected under an optical microscope for SCXRD measurement. Intensity data for single crystals **Bz-BiBrON** was collected at 100 K using graphite monochromatic MoK_α radiation ($\lambda = 0.71073 \text{ \AA}$) on a Supernova CCD diffractometer. The structure was solved by direct methods and refined by full-matrix least-

squares on F^2 using the SHELX-2018 program package.² The hydrogen atoms connected to all C atoms were located at geometrically calculated positions. The non-hydrogen atoms were refined anisotropically.

Hirshfeld surface analyses. Intermolecular interactions for **Bz-BiBrON** were analysed through Hirshfeld surface analysis via Crystal Explore 17.³⁻⁷ A crystal molecule's Hirshfeld surface is fabricated by partitioning space in the crystal into regions where the ratio of the electron density of a sum of spherical atoms for the molecule (the promolecule) is equal to 0.5. d_e is the distance from the Hirshfeld surface to the nearest nucleus outside the surface, while d_i refers to the distance from Hirshfeld surface to internal nearest nucleus. d_{norm} is the sum of d_e and d_i which are both normalized by van der Waals radii (r^{vdw}). Three colours can be observed on the Hirshfeld surface d_{norm} , namely red, white and blue. The red colour shows that the intermolecular contacts are closer than the sum of their r^{vdw} . The white colour denotes the interactions around the r^{vdw} and the blues represent the longer contacts. By plotting the distribution of points from the Hirshfeld surface, 2D fingerprint plots could be obtained, which are utilized to summarize the intermolecular interactions.⁸ On the 2D fingerprint plots, each point corresponds to a unique (d_e , d_i) pair and their colour corresponds to the contribution of the weak interactions. The blue colour refers to a small contribution to the surface, while the red colour indicates the greatest contribution.

Density Functional Theory (DFT) calculation. According to the single-crystal structure refinement results, DFT calculations of **Bz-BiBrON** was implemented in the Vienna Ab initio Simulation Package (VASP).⁹ Theoretical calculations are processed and analysed using VASPKIT.¹⁰ The generalized gradient approximation (GGA) for the exchange-correlation term with the Perdew–Burke–Ernzerhof (PBE)¹¹ exchange-correlation functional was applied for electron-electron exchange-correlation processes. To ensure sufficient accuracy, the cut-off energy of 500 eV for the plane wave expansion was chosen, self-consistent field (SCF) computations were set to a convergence criterion of 1×10^{-5} eV and the force criterion was $0.02 \text{ eV } \text{\AA}^{-1}$.

Table S1. Crystal data and structure refinement for compound **Bz-BiBrON**.

ccdc number	2414625
Empirical formula	C ₆₃ H _{64.67} Bi ₂ Br ₈ S _{2.33} N _{1.67} O ₄ P ₂
Formula weight	2103.09
Temperature/K	100(2)
Crystal system	monoclinic
Space group	<i>P2₁/c</i>
<i>a</i> /Å	15.4274(3)
<i>b</i> /Å	12.1720(2)
<i>c</i> /Å	18.5678(3)
<i>β</i> /°	95.656(2)
Volume/Å ³	3469.73(11)
<i>Z</i>	2
ρ_{calc} g/cm ³	2.013
μ /mm ⁻¹	9.833
<i>F</i> (000)	1999.0
Crystal size/mm ³	0.20 × 0.20 × 0.20
Radiation	MoK α (λ = 0.71073)
2 θ range for data collection/°	4.008 to 61.792
Index ranges	-20 ≤ <i>h</i> ≤ 21, -17 ≤ <i>k</i> ≤ 16, -24 ≤ <i>l</i> ≤ 25
Reflections collected	39784
Independent reflections	9180 [<i>R</i> _{int} = 0.0428]
Data/restraints/parameters	9180/336/424
Goodness-of-fit on <i>F</i> ²	1.098
Final <i>R</i> indexes [<i>I</i> ≥ 2 σ (<i>I</i>)]	<i>R</i> ₁ = 0.0373, <i>wR</i> ₂ = 0.0552
Final <i>R</i> indexes [all data]	<i>R</i> ₁ = 0.0506, <i>wR</i> ₂ = 0.0577

[a] $R_1 = \sum \|F_o| - |F_c|\| / \sum |F_o|$, [b] $wR_2 = [\sum w(F_o^2 - F_c^2)^2 / \sum w(F_o^2)^2]^{1/2}$

Table S2. Selected bond length (Å) and bond angle (°) for **Bz-BiBrON**.

Bi(1)-Br(1)	2.8991(4)	Bi(1)-Br(4B)	2.841(6)
Bi(1)-Br(2)	2.8026(4)	Bi(1)-O(2)	2.477(3)
Bi(1)-Br(3)	2.7383(4)	Bi(1)-O(1)	2.489(4)
Bi(1)-Br(4)	2.7422(9)	Bi(1)-O(1B)	2.440(19)

Table S3. Selected bond angles (°) for **Bz-BiBrON**.

Br(2)-Bi(1)-Br(1)	171.190(14)	O(1B)-Bi(1)-Br(1)	91.2(5)
Br(2)-Bi(1)-Br(4B)	89.38(15)	O(1B)-Bi(1)-Br(2)	80.3(5)
Br(3)-Bi(1)-Br(1)	92.671(12)	O(1B)-Bi(1)-Br(3)	88.4(6)
Br(3)-Bi(1)-Br(2)	89.238(13)	O(1B)-Bi(1)-Br(4B)	167.5(6)
Br(3)-Bi(1)-Br(4)	91.28(5)	O(1B)-Bi(1)-O(2)	94.2(6)
Br(3)-Bi(1)-Br(4B)	84.38(17)	O(2)-Bi(1)-Br(1)	91.39(6)
Br(4)-Bi(1)-Br(1)	93.54(5)	O(2)-Bi(1)-Br(2)	87.15(6)
Br(4)-Bi(1)-Br(2)	95.01(4)	O(2)-Bi(1)-Br(3)	175.14(7)
Br(4B)-Bi(1)-Br(1)	99.37(15)	O(2)-Bi(1)-Br(4)	85.81(8)
O(1)-Bi(1)-Br(1)	82.13(10)	O(2)-Bi(1)-Br(4B)	92.33(18)
O(1)-Bi(1)-Br(2)	89.06(10)	O(2)-Bi(1)-O(1)	81.15(14)
O(1)-Bi(1)-Br(3)	102.05(12)	N(1)-O(1)-Bi(1)	124.2(4)
O(1)-Bi(1)-Br(4)	166.13(13)	S(1)-O(2)-Bi(1)	125.06(16)

Table S4. Hydrogen bonds data for **Bz-BiBrON**.

D-H...A	d(D-H)/Å	d(H-A)/Å	d(D-A)/Å	<(DHA)/°
C(2)-H(2A)···Br(4)#1	0.95	3.08	3.935(6)	151.1
C(4)-H(4A)···Br(4)#2	0.95	2.76	3.601(6)	147.4
C(34)-H(34A)···Br(3)#1	0.98	3.13	3.89(3)	134.9
C(34)-H(34B)···Br(2)#1	0.98	3.01	3.68(3)	126.4
C(7)-H(7A)···Br(4)#3	0.98	2.98	3.810(5)	143.7
C(7)-H(7A)···Br(4B)#3	0.98	2.72	3.611(8)	150.8
C(8)-H(8A)···Br(4)#3	0.98	3.02	3.836(4)	142.1
C(8)-H(8A)···Br(4B)#3	0.98	3.03	3.851(7)	142.1
C(8)-H(8C)···Br(2)	0.98	2.95	3.737(5)	137.6
C(8)-H(8C)···Br(3)#1	0.98	2.98	3.503(4)	114.3
C(16)-H(16A)···Br(1)	0.95	3.10	4.050(5)	175.6
C(22)-H(22A)···Br(1)#4	0.95	3.09	4.030(4)	172.3
C(27)-H(27A)···Br(1)#4	0.99	3.07	3.999(4)	157.5
C(27)-H(27B)···Br(1)	0.99	2.74	3.716(4)	168.6

Symmetry transformations used to generate equivalent atoms:
 #1 1-x, -1/2+y, 3/2-z; #2 +x, 3/2-y, 1/2+z; #3 1-x, 1-y, 1-z; #4 -x, 1-y, 1-z.

Table S5. Hydrogen bonds data for **BiBrON**.

D-H...A	D-H (Å)	H...A (Å)	D...A (Å)	<(DHA) (°)
C(1)-H(1)···Br(3)	0.93	3.00	3.740(8)	137.5
C(2)-H(2)···Br(2)#2	0.93	3.03	3.903(7)	156.4
C(30)-H(30B)···Br(2)#3	0.96	2.95	3.820(9)	151.6
C(30)-H(30C)···Br(4)#4	0.96	2.96	3.757(10)	141.8
C(31)-H(31B)···Br(2)#3	0.96	2.96	3.797(10)	147.1
C(11)-H(11)···Br(1)#5	0.93	2.96	3.860(7)	163.9

Symmetry transformations used to generate equivalent atoms:

#1 $-x+2, -y+1, -z+1$; #2 $x, -y+3/2, z+1/2$; #3 $-x+2, -y+1, -z$; #4 $-x+2, y-1/2, -z+1/2$; #5 $x, -y+1/2, z+1/2$.

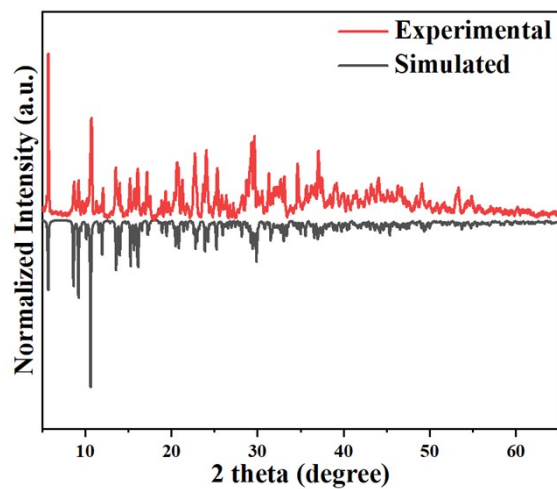


Figure S1 The simulated and experimental PXRD patterns of **Bz-BiBrON** after storing at ambient conditions for 10 months.

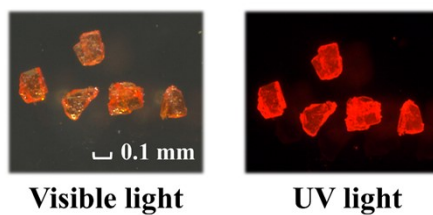


Figure S2 **Bz-BiBrON** single crystal daylight photo and UV light photo.

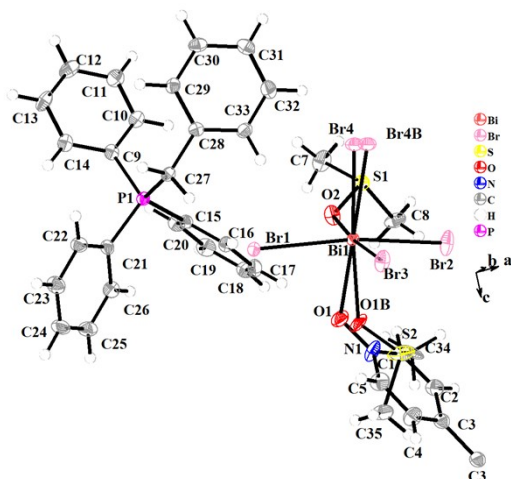


Figure S3. ORTEP drawing (50% ellipsoid probability) of the asymmetric unit of **Bz-BiBrON**.

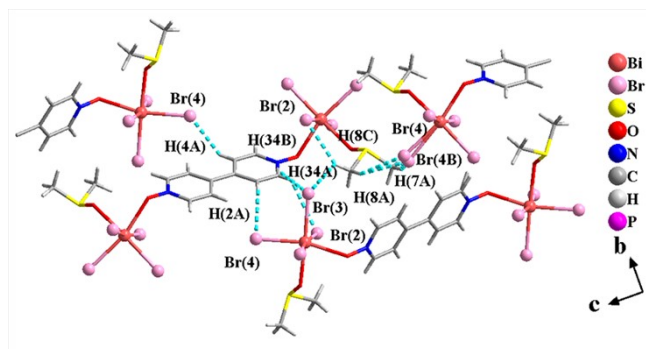


Figure S4. A schematic diagram showing hydrogen bonds (cyan dotted lines) among anion units in **Bz-BiBrON**.

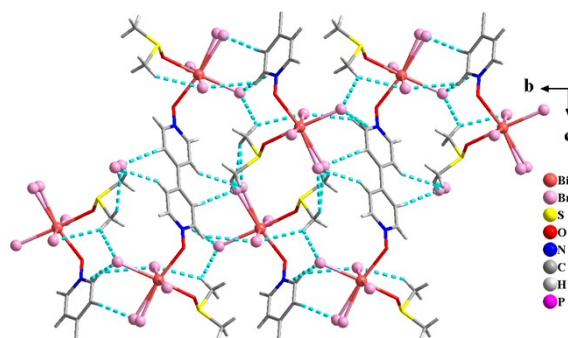


Figure S5. A diagram showing the hydrogen bonding (cyan dot line) within the anion layer of **Bz-BiBrON**.

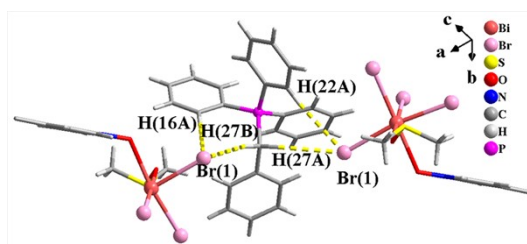


Figure S6. A diagram showing the hydrogen bonding (yellow dotted line) between the anion and cation units of **Bz-BiBrON**.

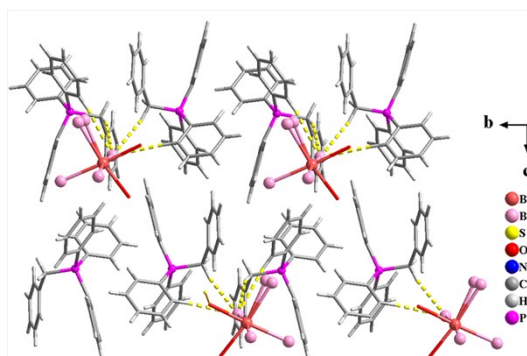


Figure S7. A diagram showing the hydrogen bonding (yellow dotted line) of the anion and cation layers in **Bz-BiBrON**.

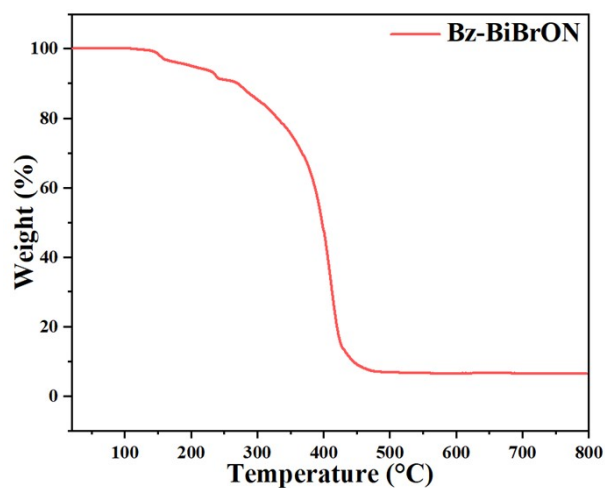


Figure S8. The thermogravimetric curve for **Bz-BiBrON**.

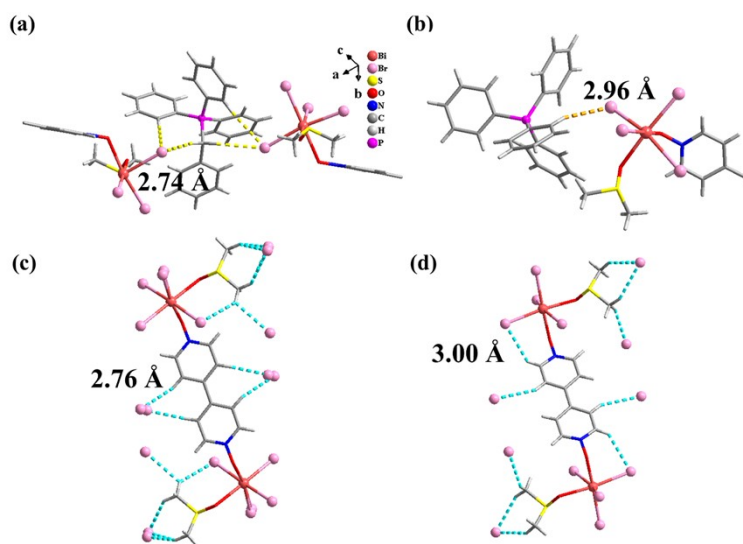


Figure S9. The hydrogen bonding and the shortest distance (yellow lines) between anions and cations in **Bz-BiBrON** and **BiBrON** compounds are shown in (a) and (b). The hydrogen bonds and the shortest distances (blue lines) around the ligands in **Bz-BiBrON** and **BiBrON** compounds are shown in (c) and (d), respectively.

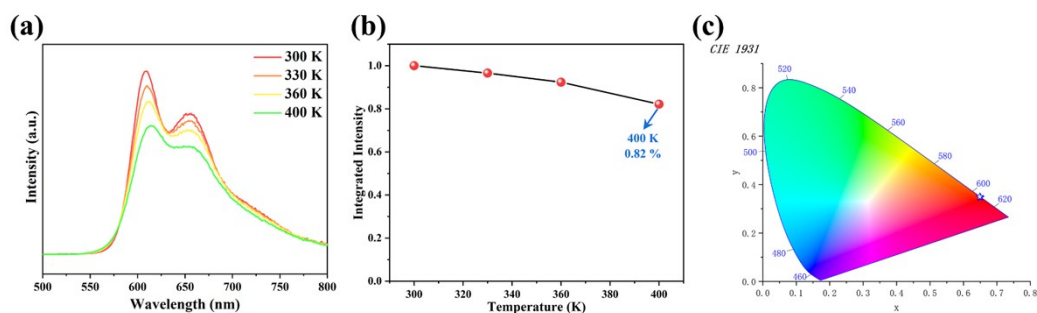


Figure S10 a) Temperature-dependent PL spectra of **Bz-BiBrON** under 430 nm excitation at 300 K to 400 K. b) Integrated intensity for PL of **Bz-BiBrON** at different temperatures ranging from 300 to 400 K. c) CIE chromaticity coordinates of **Bz-BiBrON** in the range of 300 ~ 400 K.

1. C. F. Macrae, I. Sovago, S. J. Cottrell, P. T. A. Galek, P. McCabe, E. Pidcock, M. Platings, G. P. Shields, J. S. Stevens, M. Towler and P. A. Wood, *J. Appl. Crystallogr.*, 2020, **53**, 226-235.
2. G. M. Sheldrick, *Acta Crystallogr. C Struct. Chem.*, 2015, **71**, 3-8.
3. J. J. McKinnon, M. A. Spackman and A. S. Mitchell, *Acta Crystallogr. Sect. B-Struct. Sci. Cryst. Eng. Mat.*, 2004, **60**, 627-668.
4. J. J. McKinnon, D. Jayatilaka and M. A. Spackman, *Chem. Commun.*, 2007, 3814-3816.
5. M. A. Spackman, J. J. McKinnon and D. Jayatilaka, *CrystEngComm*, 2008, **10**, 377-388.
6. M. A. Spackman and D. Jayatilaka, *CrystEngComm*, 2009, **11**, 19-32.
7. M. J. Turner, J. J. McKinnon, D. Jayatilaka and M. A. Spackman, *CrystEngComm*, 2011, **13**, 1804-1813.
8. M. A. Spackman and J. J. McKinnon, *CrystEngComm*, 2002, **4**, 378-392.
9. G. Kresse and J. Furthmuller, *Comput. Mater. Sci.*, 1996, **6**, 15-50.
10. V. Wang, N. Xu, J. C. Liu, G. Tang and W. T. Geng, *Comput. Phys. Commun.*, 2021, **267**, 19.
11. J. P. Perdew, K. Burke and M. Ernzerhof, *Phys. Rev. Lett.*, 1996, **77**, 3865-3868.